Electrochemical performance of patterned $LiFePO_4$ nano-electrode with a pristine amorphous layer

Mao Wang, Wei Zhang, Yihang Liu, Yong Yang, Chunsheng Wang, and Yuan Wang

Citation: Appl. Phys. Lett. **104**, 171604 (2014);
View online: https://doi.org/10.1063/1.4873581
View Table of Contents: http://aip.scitation.org/toc/apl/104/17
Published by the American Institute of Physics

Electrochemical performance of patterned $LiFePO_4$ nano-electrode with a pristine amorphous layer

Mao Wang,[1] Wei Zhang,[2] Yihang Liu,[3] Yong Yang,[1] Chunsheng Wang,[3,a)] and Yuan Wang[1,a)]

[1]*Key Laboratory of Radiation Physics and Technology, Ministry of Education, Institute of Nuclear Science and Technology, Sichuan University, Chengdu 610064, People's Republic of China*
[2]*Analytical and Testing Center, Sichuan University of Science and Engineering, Zigong, Sichuan 643000, People's Republic of China*
[3]*Department of Chemical and Biomolecular Engineering, University of Maryland, College Park, Maryland 20742, USA*

(Received 19 March 2014; accepted 11 April 2014; published online 29 April 2014)

A patterned $LiFePO_4$ nanorod with a pristine amorphous $LiFePO_4$ surface layer was fabricated by controlling the temperature gradient from the interior to the exterior layer in high-temperature annealing process through designing hierarchical multilayer electrode structure. The three dimensional patterned $LiFePO_4$ nanorods were prepared using tobacco mosaic virus nanoforest arrays. The results indicate that the nano-electrodes nearly reached the theoretical capacity at a very low C rate even without conductive coatings. The amorphous $LiFePO_4$ can fast transport the Li-ion to inside crystal $LiFePO_4$, thus enhancing the rate capability. © *2014 AIP Publishing LLC*. [http://dx.doi.org/10.1063/1.4873581]

The olivine-type $LiFePO_4$ has been considered as one practical choice for lithium-ion battery electrodes material due to its superior inherent merits, including low cost, environment friendliness, remarkable thermal stability, excellent long cycle ability, and high safety.[1] However, the application of $LiFePO_4$ is limited because of its poor high C rate performance, which is restricted by sluggish kinetics of electron[2] and Li^+ transport.[3]

The challenge of poor power density can be migrated when the $LiFePO_4$ electrodes is fabricated as three-dimensional (3-D) nano-array[4] and coated with a superior ionic/electronic conductor layer on $LiFePO_4$ nano-array surface. For example, highly electronic conductive carbon was coated on the surface of $LiFePO_4$ for improving surface conductivity.[5] However, the carbon may decrease the tap density of materials[6] and introduce the impurity contamination when the battery is applied in micro-electromechanical systems (MEMS).

Alternatively, highly conductive amorphous glass film was also coated to nanostructured $LiFePO_4$ to enhance the power density. For example, as a conductive and protective layer, the amorphous conductive NiP and glassy lithium phosphate phase[7] layer were coated on $LiFePO_4$ to enhance the rate performance of $LiFePO_4$.[8] The amorphous $Li_4P_2O_7$ coated on the $LiFePO_4$ surface could improve the ionic conductivity, thus enhance rate capacity of electrodes.[9] It is suggested[10] that the disordered nature of the amorphous materials can also modify the surface potential of lithium to facilitate the adsorption of Li^+.

However, it has been a challenge to design a robust heterogeneous surface films on the electrode that surviving in entire life of batteries even though the advantages of these surface films are well understood.[11] The fabrication of amorphous binary or ternary compounds usually involved some complicated synthesis process.[8–11] Since heterogeneous layer normally has different compositions with the underneath electrode, the interface between surface heterogeneous layer and cathode may withstand the inevitable thermal flux during the micro-fabrication process and subsequent charge-discharge cycle, resulting in increase of interface resistance,[12] thus decrease the electrochemical properties of cathode materials.[13]

In this Letter, the 3-D multilayer $LiFePO_4$ nano-electrodes were prepared by using the tobacco mosaic virus (TMV1cys) as the templates. A pristine amorphous layer (PAL) of the $LiFePO_4$ was formed on the surface of nano-$LiFePO_4$ electrodes by designing a hierarchical architecture of multilayer $LiFePO_4$ thin films. Since the PAL has the same composition with the electrode, thus significantly reduces the interface resistance. The effects of the pristine amorphous surface toplayer on electrochemical properties of 3-D $LiFePO_4$ nano-electrode were systematically investigated.

The self-assembly TMV1cys was adopted as a bioinorganic template to form nano-scaled 3-D structure.[14] To form an amorphous $LiFePO_4$ layer on the crystal $LiFePO_4$ electrode, a temperature gradient range from the interior to the outmost surface of $LiFePO_4$ during annealing in a vacuum chamber was created by designing multilayer thin films with different thermal conductivities. Since the thermal radiation in the vacuum chamber is very weak, the temperature gradient can be created by the inside-out thermal conduction of multilayer films, which can induce a successive phase transformation in the as-prepared $LiFePO_4$ cathodes.[15]

The Titanium (Ti) and Nickel (Ni) films were employed as thermal conductive layers. The Ni films were deposited on TMV1cys templates well by the electroless plating method. The highly dense Ni/TMV1cys nanorods were attached to the SS substrate in a nearly vertical manner (Fig. 1(a)). Since Ni atom could rapidly drift into the $LiFePO_4$ film during charge-discharge cycles procedure[16] reducing the electrochemical performance of $LiFePO_4$, Ti barrier layers were

a)Authors to whom correspondence should be addressed. Electronic addresses: cswang@umd.edu and wyuan@scu.edu.cn

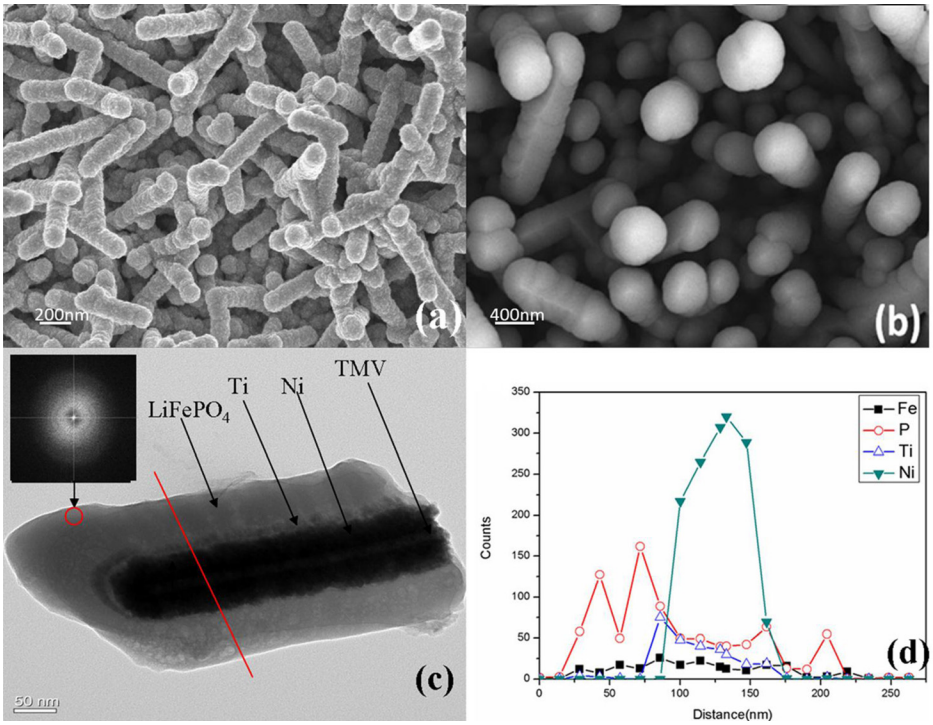

FIG. 1. (a) SEM image of Ti/Ni/TMV; (b) SEM image of as-deposited 3-D $LiFePO_4$/Ti/Ni/TMV; (c) TEM image of single 3-D $LiFePO_4$/Ti/Ni/TMV electrode and corresponding FFT (Fast Fourier Transform) figure; (d) EDS element line distribution of single electrode along the red line in (c).

deposited between Ni and $LiFePO_4$ layers for preventing the Ni diffusion. Moreover, the tensile strength of Ti (about 240 MPa (Ref. 17)) is relatively higher. The integration of Ti and Ni metal layers can also improve the electric contact of layer interfaces and the rigidity of the electrodes, which can effectively accommodate the stress/strain generated between electrode and the substrate due to the volume change of the electrodes during lithiation-delithiation process, and thus improving the stability of cathodes. The deposition of Ni, Ti, and $LiFePO_4$ layers in sequence can therefore form the hierarchical architecture of multilayer films with different thermal conductivities.

The magnetron sputtering deposition of $LiFePO_4$ on 3-D Ti/Ni/TMV substrates was conducted in base pressure of 1.5×10^{-4} Pa and working pressure of 1 Pa at a sputtering power density of 3 W/cm^2. The average deposition rate is 4.5 nm/min. The target-to-substrate distance is 70 mm. The surface morphology of 3-D $LiFePO_4$/Ti/Ni/TMV1cys electrodes is shown in Fig. 1(b). After sputtering deposition, some samples were annealed at 500 °C for either 2 h or 4 h in a vacuum furnace. The pressure of the vacuum furnace was lower than 1.0×10^{-3} Pa during annealing.

X-ray diffraction (XRD) measurement was employed to ascertain the crystallographic structure of the samples by a Rigaku diffractometer using Cu-Kα radiation. Mass of samples was weighed by a high precision microbalance with an accuracy of 1 μg before and after $LiFePO_4$ depositing. The surface morphology of nano-electrodes was observed by Field Emission Scanning Electron Microscope (FESEM). A high-resolution transmission electron microcopy (HRTEM) with an energy-dispersive spectrometer (EDS) was employed to analyze the microstructures and composition of nano-electrodes. The electrochemical performance of $LiFePO_4$/Ti/Ni/TMV nano-electrodes was evaluated using coin cells (R2032) with lithium foil as an anode electrode and a 1M $LiPF_6$ solution in ethylene carbonate/diethyl carbonate (1:1 by volume) as an electrolyte.

The as-deposited $LiFePO_4$/Ti/Ni/TMV nanorods have an average of ~500 nm in diameter and greater than 2.5 μm in length (Fig. 1(b)). The microstructure of $LiFePO_4$, Ti, and Ni layers can be clearly identified by EDS line scan and TEM images as shown in Figs. 1(c) and 1(d). These results indicate that the $LiFePO_4$/Ti/Ni/TMV nano-electrodes were constructed.

The XRD patterns of the $LiFePO_4$/Ti/Ni/TMV nano-electrodes are shown in Fig. 2. The as-deposited $LiFePO_4$ nano-electrodes give no apparent diffraction peaks as shown in Fig. 2(a), which is in accordance with an amorphous ring in the interpolated FFT image as shown in the insetted image of Fig. 1(c). It is clear that the as-deposited nano-electrodes have amorphous structure. After annealed at 500 °C for 2 h or 4 h, all the diffraction peaks of the nano-electrodes (Figs. 2(b) and

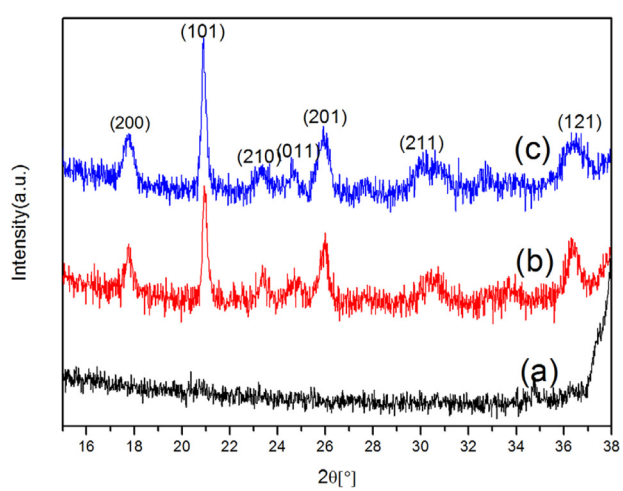

FIG. 2. XRD patterns of $LiFePO_4$ cathodes. (a) As-deposited multi-layers; (b) annealed at 500 °C for 2 h in vacuum; (c) annealed at 500 °C for 4 h in vacuum.

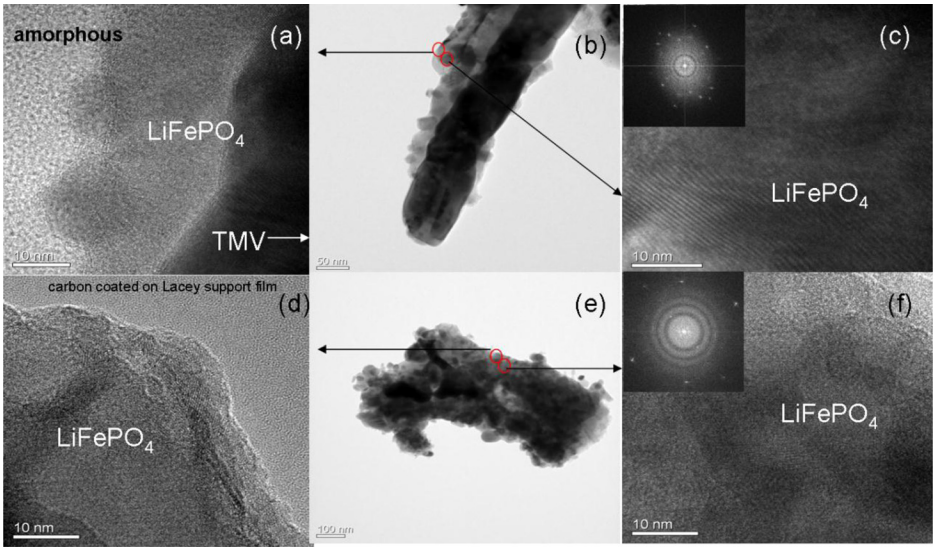

FIG. 3. (a) HRTEM image of (b); (b) TEM image of 3-D $LiFePO_4$ nano-electrode with a pristine amorphous layer; (c) HRTEM image of (b) and corresponding SAED pattern; (d) HRTEM image of (e); (e) TEM image of 3-D $LiFePO_4$ nano-electrode with full crystal structure; (c) HRTEM image of (e) and corresponding SAED pattern.

2(c)) can be indexed to the orthorhombic system with the Pnma space group, according to the JCPDF database. No diffraction peaks related with Ni and Ti are observed in Fig. 2 because the thickness of the metal sub layer is too thin.

Fig. 3 shows the microstructure of the annealed nano-electrodes. As demonstrated in the FFT and TEM images (Figs. 3(a)–3(c)), a 10 nm PAL was coated on the outmost surface of the nano-electrodes that were annealed at 500 °C for 2 h. Therefore, the PAL could be grown on the outmost surface of the crystal $LiFePO_4$ nano-electrodes when the LiFePO4/Ti/Ni/TMV nano-electrode was annealed at 500 °C for 2 h. However, the nano-electrodes were completely crystallized with further increasing annealing time (Figs. 3(d)–3(f)). Therefore, the PAL can be formed on the outermost surface of nano-electrodes by tuning the annealing process. This is because the heat transmission of multilayer nano-electrodes during annealing process is along the sub-layer metal (Ti and Ni) from inside to outside generate a temperature gradient ranging from the interior to the exterior layer of multilayer films. The crystallization of $LiFePO_4$ would start in sequence along the depth direction of the multilayer films. Therefore, the multilayer $LiFePO_4$/Ti/Ni/TMV nano-electrodes with either the pristine amorphous toplayer or full crystal structure (FC) layer can be obtained simply by the precise control of annealing parameters.

Fig. 4(a) shows the charge/discharge voltage profiles of $LiFePO_4$ nano-electrodes with the PAL and FC at 1C. As shown in Fig. 4(a), both charge and discharge profiles show reversible electrochemical reactions at voltage plateaus around 3.4 V, which are the characteristic of phase transition between $FePO_4$ and $LiFePO_4$. Without adding conducting materials, both the $LiFePO_4$ multilayer nano-electrodes could nearly reach the theoretical value at 0.1C as showing in Fig. 4(b). To evaluate the effects of the crystal structure of surface layer on rate performance, both $LiFePO_4$ nano-electrodes with crystal and amorphous surface layer were subjected to an aggressive testing protocol in which the cells were both charged and discharged at the same rate. Fig. 4(b) shows the rate capacity of the two $LiFePO_4$/Ti/Ni/TMV electrodes at different charge/discharge current rates from 0.1C to 10C.

The capacity of both electrodes at 0.5C dropped down 14% and 18% than those of nano-electrodes at 0.1C, respectively. However, due to the fast Li-ion transport in amorphous $LiFePO_4$, the discharge capacity of the $LiFePO_4$ nano-electrodes with PAL is higher than that of the nano-electrodes with FC when the cycling is larger than 1C rate (Fig. 4(b)). Moreover, the discharge capacity of the $LiFePO_4$ nano-electrodes with PAL was 12.5% and 24% higher than those of the $LiFePO_4$ nano-electrodes with FC at 5C and 10C, respectively (Fig. 4(b)). Even after a certain number of charge/discharge cycles at 5C and 10C, the $LiFePO_4$ nano-electrodes with PAL had a slower capacity fading rate and a better high-rate charge-discharge cycle performance (Fig. 4(b)). This might be explained by that the PAL removes the anisotropy of the surface properties[18] and enhances the delivery of Li^+ to the (010) facet of $LiFePO_4$

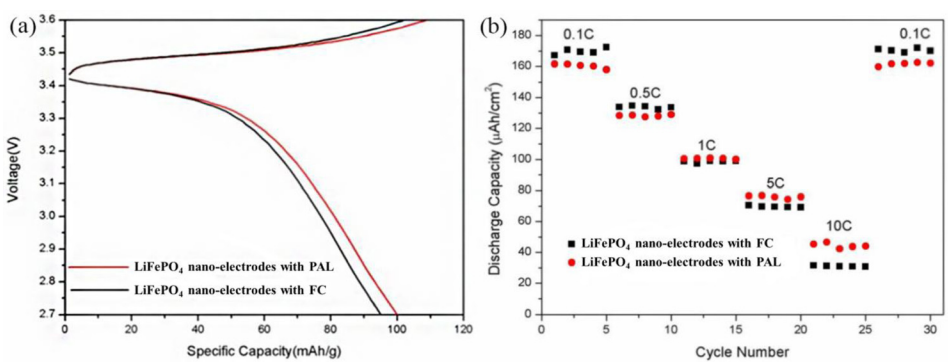

FIG. 4. The electrochemical characterizations of the 3-D $LiFePO_4$ nano-electrodes. (a) Charge–discharge curve at 1C; (b) the specific capacities at different rates.

where it can be inserted. It is concluded that the limiting factor for charge/discharge is the delivery of Li^+ and electrons at the surface diffusion rather than bulk diffusion. Therefore, the high-rate discharge performance of the materials can be improved by coating $LiFePO_4$ with the PAL, which can eliminate the anisotropy of the surface and increase the diffusion rate of the lithium ion in electrode material surface.

In conclusion, we have prepared the 3-D $LiFePO_4$/Ti/Ni/TMV nano-electrodes. A pristine amorphous surface toplayer on 3-D $LiFePO_4$ nano-electrode was formed by one-step annealing process through designing a hierarchical architecture of multilayer thin films. The effects of PAL and FC surface layers on electrochemical performance of the $LiFePO_4$ nano-electrodes were systematically investigated. Both of the $LiFePO_4$ nano-electrodes can nearly reach the theoretical capacity at a low C rate without coating conducting materials. However, the $LiFePO_4$ cathode with PAL has a predominant rate capacity at high C rate and a slower capacity fading rate. The pristine amorphous surface structure of the nano-electrodes can significantly enhance the rate performance of the lithium-ion battery.

This study was supported by National Natural Science Foundation of China (Grant No. 51171124), Scientific and Technical Supporting Programs funded by Science and Technology Department of Sichuan Province (Nos. 2014GZ0004 and 2011GZ0187), and the Program for New Century Excellent Talents in University (Grant No. NCET-08-0380).

[1]A. K. Padhi, K. S. Nanjundaswamy, and J. B. Goodenough, J. Electrochem. Soc. **144**, 1188 (1997).
[2]A. K. Padhi, K. S. Nanjundaswamy, C. Masquelier, S. Okada, and J. B. Goodenough, J. Electrochem. Soc. **144**(5), 1609 (1997).
[3]C. Sun, S. Rajasekhara, J. B. Goodenough, and F. Zhou, J. Am. Chem. Soc. **133**(7), 2132 (2011).
[4]Y. Liu, W. Zhang, Y. Zhu, Y. Luo, Y. Xu, A. Brown, J. N. Culver, C. A. Lundgren, K. Xu, Y. Wang, and C. Wang, Nano Lett. **13**(1), 293 (2013).
[5]Y. Wu, Z. Wen, and J. Li, Adv. Mater. **23**(9), 1126 (2011).
[6]J. Wang and X. Sun, Energy Environ. Sci. **5**(1), 5163 (2012).
[7]B. Kang and G. Ceder, Nature **458**(7235), 190 (2009).
[8]G.-M. Song, Y. Wu, Q. Xu, and G. Liu, J. Power Sources **195**(12), 3913 (2010).
[9]A. Kayyar, H. Qian, and J. Luo, Appl. Phys. Lett. **95**(22), 221905 (2009).
[10]N. Meethong, Y.-H. Kao, M. Tang, H.-Y. Huang, W. Craig Carter, and Y.-M. Chiang, Chem. Mater. **20**(19), 6189 (2008).
[11]K.-S. Park, A. Benayad, M.-S. Park, A. Yamada, and S.-G. Doo, Chem. Commun. **46**(15), 2572 (2010).
[12]J. Luo, M. Tang, R. M. Cannon, W. Craig Carter, and Y.-M. Chiang, Mater. Sci. Eng., A **422**(1–2), 19 (2006).
[13]M. Saiful Islam, D. J. Driscoll, C. A. J. Fisher, and P. R. Slater, Chem. Mater. **17**(20), 5085 (2005).
[14]X. Chen, K. Gerasopoulos, J. Guo, A. Brown, C. Wang, R. Ghodssi, and J. N. Culver, ACS Nano **4**(9), 5366 (2010).
[15]J. Svoboda, E. Gamsjäger, F. D. Fischer, and P. Fratzl, Acta Mater. **52**(4), 959 (2004).
[16]K.-F. Chiu, J. Electrochem. Soc. **154**(2), A129 (2007).
[17]M. Niinomi, Mater. Sci. Eng., A **243**(1–2), 231 (1998).
[18]L. Wang, F. Zhou, Y. S. Meng, and G. Ceder, Phys. Rev. B **76**(16), 165435 (2007).